

1.6 NEW METHOD FOR THE DETERMINATION OF TURBULENT SURFACE FLUXES FROM LOW-LEVEL FLIGHTS: VERIFICATION AND BENEFIT IN JOINT FIELD EXPERIMENTS

Jens Bange, Thomas Spieß, and Peter Zittel

Aerospace Systems at Technical University Braunschweig, Germany

1. INTRODUCTION

The determination of area-averaged vertical turbulent fluxes of heat, humidity, and momentum at surface level in the framework of a joint field experiment is an useful task for several reasons. E.g., the measured area-averaged fluxes act as ground-truth data for remotely sensed data. This ground-truth is also the base for the development of averaging strategies of ground-based point measurements in a heterogeneous terrain. Large eddy simulations (LES) can be initialized or verified, as well as forecast models. The knowledge achieved from the analysis of turbulent fluxes under various terrain and synoptic conditions helps to improve the numerical weather prediction as well as the climate models.

Generally aircraft are very suitable instruments to measure area-averaged turbulent fluxes. For the determination of the mean surface heat flux in a convective boundary layer (CBL), the usual method is to fly square-shaped flight patterns at at least three different altitudes within the CBL (3D pattern or 3D-box flights, see Fig. 1). At each flight level z_f the area-averaged flux (in this example the vertical flux of sensible heat) is determined by

$$H(z_f) = \frac{1}{n} \sum_{i=1}^n \rho c_p \langle w' \theta' \rangle, \quad (1)$$

where ρ is the air density and c_p the specific heat capacity of air. The turbulent fluctuations w' and θ' of the vertical wind and the potential temperature, respectively, are averaged ($\langle \dots \rangle$) only over straight flight sections (legs). Applying the box flight pattern, the number of legs $n = 4$. Assuming a linear heat flux profile in the CBL the area-averaged fluxes are then extrapolated to the ground.

The drawbacks of this method are obvious: First, flights at minimum three different altitudes are necessary, which consumes time and money.

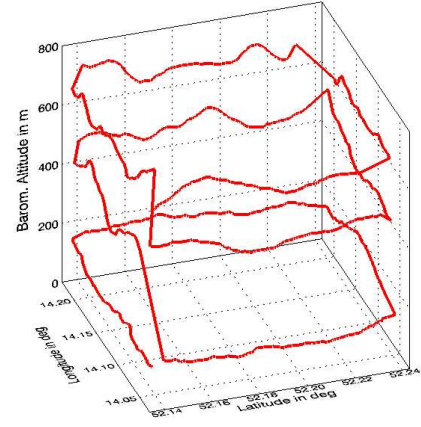


Fig. 1: 3D flight pattern

Second, for the time of flights stationarity or at least a linear temporal development of the CBL must be assumed. And third, a linear flux profile through the entire atmospheric boundary layer (ABL) must be assumed, which is not problematic for the heat fluxes in a CBL, but unlikely for momentum and latent heat near the surface and for other types of thermal stratification.

Grunwald *et al.* 1998 introduced the low-level flight method (LLF) to determine the surface fluxes from flights at only one low altitude by solving the budget equation. For the turbulent sensible heat flux H , this is:

$$\frac{1}{\rho c_p} \cdot \frac{\partial H}{\partial z} = -\frac{\partial \bar{\theta}}{\partial t} - \left(\bar{u} \frac{\partial \bar{\theta}}{\partial x} + \bar{v} \frac{\partial \bar{\theta}}{\partial y} \right), \quad (2)$$

where \bar{u} and \bar{v} are the mean horizontal wind velocities, and $\bar{\theta}$ is the mean potential temperature.

The LLF strategy consumes less flight time and has therefore big advantages compared to the 3D method. Of course assumptions for the vertical profiles of the fluxes between the surface and the flight level have to be made further on. And the LLF method requires additional measurements with e.g. ground-based systems to receive the horizontal gradients and the temporal development of temperature, humidity, and wind. Therefore with the LLF method an airborne system can not be used autonomously but depends on supporting systems.

Corresponding author: Jens Bange, Aerospace Systems, Technical University of Braunschweig, Germany; e-mail: j.bange@tu-bs.de



Fig. 2: The helicopter-borne turbulence measurement system Helipod is an autonomously operating sensor system, attached to a 15 m rope. It operates at 40 ms^{-1} air speed and measures wind vector, temperature, and humidity at a rate of 100 Hz.

2. THE INVERSE METHOD

To obtain a stand-alone procedure the low-level flights were combined with the inverse theory (e.g., Tarantola 1987) to calculate the missing parameters in the budget equations. The inverse modeling technique uses a measured data set \vec{d}_{obs} of an atmospheric quantity and an assumed model relationship G that describes physical processes of the quantity to reproduce the measured data as a set of parameters \vec{m} (Wolff and Bange 2000). In other words the technique uses appropriate model assumptions that are based on theoretical assumptions to fit measured data. For the energy budget (2) we assumed a linear relationship (linear operator G) between the model parameters \vec{m} and the measurements \vec{d}_{obs} :

$$\begin{aligned} \vec{d}_{obs} &= G(\vec{m}) \\ &= m_0 + m_1 \vec{x} + m_2 \vec{y} + m_3 \vec{z} + m_4 \vec{t} \end{aligned} \quad (3)$$

with

$$(m_1, \dots, m_4) = \left(\frac{\partial \vec{d}_{obs}}{\partial x}, \dots, \frac{\partial \vec{d}_{obs}}{\partial t} \right). \quad (4)$$

In this equation, \vec{x} , \vec{y} , and \vec{z} are Cartesian coordinates and \vec{t} is the time.

For the turbulent sensible heat flux H , the data $\vec{d}_{obs}(x, y, z)$ represent the measured potential temperature θ . To reproduce the potential temperature, the inverse model was initialized with a realistic range of values of the mean potential temperature gradient and the mean temporal development of θ . These values had to be estimated

from the synoptic situation. Then the measurement errors (the statistical uncertainties of the sensors and the probing strategy) were taken into account.

The output \vec{m} of the inverse model then provided the gradient and the temporal development of the mean potential temperature. The vertical gradient of the heat flux was then calculated by inserting the parameters \vec{m} from the inverse model output into the budget equation (2). Finally the surface heat flux was calculated by integration (2) assuming a linear profile of H :

$$H_0 = H(z_f) - z_f \cdot \frac{\partial H}{\partial z}, \quad (5)$$

with flight level z_f .

Thus the combination of low-level flights with an inverse model (LLF+IM) allows the determination of the area-averaged turbulent surface fluxes from square-shaped flight patterns at only one low altitude (e.g. at z_f 100 m or less) without any supporting data from other systems.

In the following the area-averaged sensible surface heat fluxes calculated with the LLF+IM method were compared to those obtained from 3D-box flights during the LITFASS-98 experiment, from ground-based measurements, and from simulated flight measurements in a LES.



Fig. 3: The research aircraft Do 128 recently received new equipment. The aircraft operates at an air speed of 60 m/s and samples data at 100 Hz.

3. SIMULATED FLIGHT MEASUREMENTS

Simulated flight measurements over homogeneous and heterogeneous terrain in a LES (Schröter *et al.* 2000) were consulted to verify the LLF+IM method. Area- and time-averaged turbulent fluxes were derived directly from the LES

model. These 'true' data were then used to quantify statistical and systematic errors of the inverse method. In the following example data from a LES over a heterogeneous surface are presented.

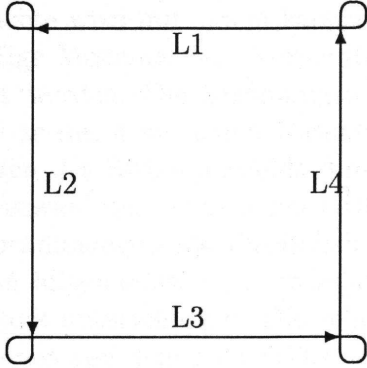


Fig. 4: Box with 4 Legs

The analysis started with the calculation of the area- and time-averaged turbulent fluxes at every grid level of the LES. The results are drawn as colored curves in Fig. 5. Within the LES model virtual measurement flights at five altitudes within the artificial CBL were performed using a square-shaped pattern (3D box, see Fig. 4). Each square was flown nine times, to meet the average time of the LES. For each square the vertical turbulent heat flux H was calculated using (1) with $n = 4 \times 9$, as well as its statistical error (Lenschow *et al.* 1994; Bange *et al.* 2002). The results are depicted as black error bars in Fig. 5. For each flight altitude the vertical gradient of the flux H was calculated using the LLF+IM method and plotted into Fig. 5 as black dashed lines. The diagram shows clearly that there were no systematic differences between LES 'true' fluxes and 'airborne measured' fluxes. The error bars of the latter were quite large, but the method to calculate these errors was not optimum at the time of the data analysis and will be improved soon. The extrapolation of the airborne measurements to the ground using LLF+IM meets the LES surface heat flux. The accuracy of the LLF+IM increases with decreasing flight altitude as expected. For the lowest flight at 100 m, the difference between 'true' and estimated surface flux was less than 2 W m^{-2} . This shows that the LLF+IM is a reliable method.

Comprising the parameters of the LES and the virtual flights:

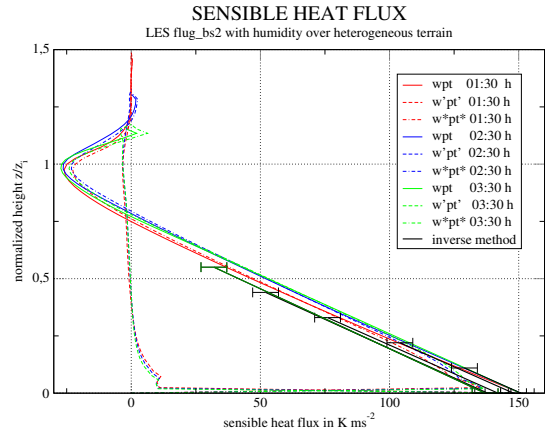


Fig. 5: Comparison of the area-averaged turbulent fluxes calculated from virtual flights (black error bars) with the 'true' data from LES. The area- and time-averaged LES fluxes are depicted by colored curves (with 1 hour time offset each) as follows: solid lines: the total sensible heat; long dashed lines: the sensible heat flux resolved by the LES; short dashed lines: the sub-scale sensible heat flux parameterized by the LES. The extrapolation of the flight measurements to the ground using the LLF+IM method is depicted by black dashed lines for each flight altitude.

- LES area: $12 \text{ km} \times 12 \text{ km}$, heterogeneous
- Horizontal grid spacing: 40 m
- Vertical grid spacing: 20 m
- Maximum model height: 1200 m
- CBL height $z_i = 950 \text{ m}$
- Stratification: slightly instable
- Sensible surface heat flux 151 W/m^2
- LES contained humidity (without condensation)
- Flights began after 90 minutes simulated time
- Flight pattern: horizontal square-shaped patterns at 5 altitudes, repeated 9 times
- 800 measurements points per square in 40 m distance
- Leg length: 8 km
- Air speed: 40 ms^{-1}
- Flight levels at 100, 200, 300, 400, 500 m

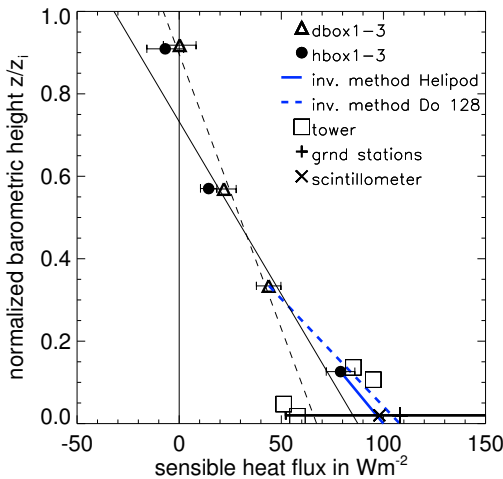


Fig. 6: Sensible heat fluxes measured in LITFASS-98. Do 128 and Helipod measurements are represented by triangles and circles, respectively. The interpolations of the 3D-box flight patterns are depicted as black thin lines. The extrapolation using the LLF+IM method is displayed by thicker blue lines (dashed: Do 128; solid: Helipod measurements, respectively).

4. LITFASS-98 MEASUREMENTS

During the LITFASS-98 experiment (Beyrich *et al.* 2002) airborne measurements using the helicopter-borne turbulence probe Helipod (Fig. 2; Bange and Roth 1999) and the research aircraft Do 128 (Fig. 3; Hankers 1989; Corsmeier *et al.* 2001) were performed to determine area-averaged vertical turbulent fluxes. Both systems are owned by the University of Braunschweig and equipped with sophisticated sensors to measure turbulent fluctuations and fluxes very precisely. The experimental site near the meteorological observatory at Lindenbergs / Germany was characterized by its strong heterogeneity.

For the Helipod a square-shaped relatively small flight pattern of 10 km x 10 km was chosen, while the Do 128 flew on a 15 km x 15 km pattern. This geometry was chosen to meet the ratio of air-speed (Helipod: 40 ms⁻¹, Do 128: 60 ms⁻¹) and to achieve simultaneous flights at three altitudes above the heterogeneous site (Fig. 1). The lowest flight level was at 140 m altitude for the Helipod and at 245 m for the Do 128. The other two common levels were located at 490 m and 760 m. During the flights the boundary layer height was between $z_i = 600$ and 800 m. The flights,

a comparison with ground-based stations, wind-profiler/RASS, tower, and scintillometer measurements, and a demonstration of the reliable results are given by Bange *et al.* (2002) and Engelbart and Bange (2002).

The Fig. 6 shows a collection of all involved instruments for the afternoon of 18 June, 1998. The interpolation of the 3D-box pattern led to different vertical gradients of the vertical turbulent heat flux, and therefore to different extrapolated surface heat fluxes. While the differences between the two airborne systems were not that large compared to the statistical errors of the ground-based systems, the analysis of the lowest flights of the Helipod and the Do 128 yield even better results: With the LLF+IM method very similar vertical gradients of the heat flux were calculated for both airborne systems. With only a small discrepancy of less than 10 Wm⁻² to each other, the extrapolated lines calculated with LLF+IM matched the ground-based micrometeorological stations and the scintillometer, as well as the upper tower measurements.

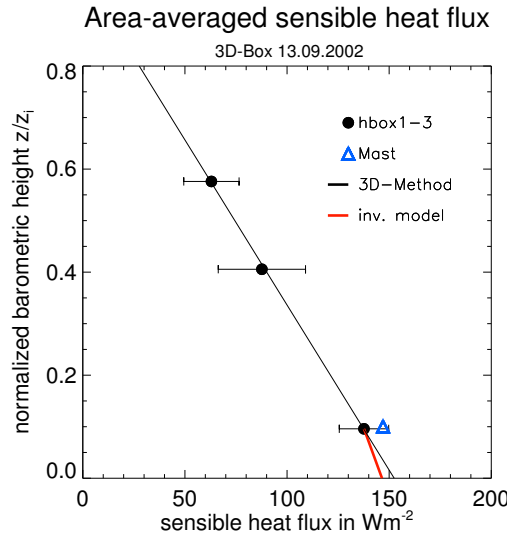


Fig. 7: Sensible surface heat fluxes measured with the Helipod (filled circles) and a 99 m tower (blue triangle) during the LIDAR-Autumn-Campaign. The black lines depicts the linear interpolation of the results from the 3D-box flight. The short red line displays the results yielded from the application of the LLF+IM method to only the lowest flight level.

When using the 3D-box method the calculations of the surface fluxes are dependent on the development of the ABL height z_i since atmospheric quantities scale with it (Deardorff scaling). Since

the determination of z_i is usually not very accurate, this adds an uncertainty to the calculation of the surface fluxes. The low-level method has the advantage of not requiring the knowledge of the boundary-layer height. A more detailed analysis of the fluxes and the methods is given by Zittel *et al.* (2002) and Zittel *et al.* (2003).

5. LIDAR-AUTUMN-CAMPAIGN 2002

The LIDAR-Autumn-Campaign in 2002 was carried out at the same site as the LITFASS-98 experiment. The goal of this short experiment, whose analysis and evaluation is on the way, was the comparison of vertical latent heat fluxes measured by a DIAL (a differential absorption LIDAR) and the Helipod. The data shown here were derived from a 3D-box flight pattern performed in a CBL. Since the DIAL was not able to measure the sensible heat flux and the humidity fluxes were not yet analyzed by the time of writing, the Helipod measurements were compared with the 99 m tower of the Lindenberg site (Fig. 7). Again there is a clear discrepancy between the vertical gradient of the flux calculated by linear interpolation of the 3D-box results and the LLF+IM method. But since the lowest flight was close to the surface, the extrapolated surface fluxes differed less than 10 Wm^{-2} to each other. The mast measurement was within the error bar of the Helipod measurement at about 100 m altitude.

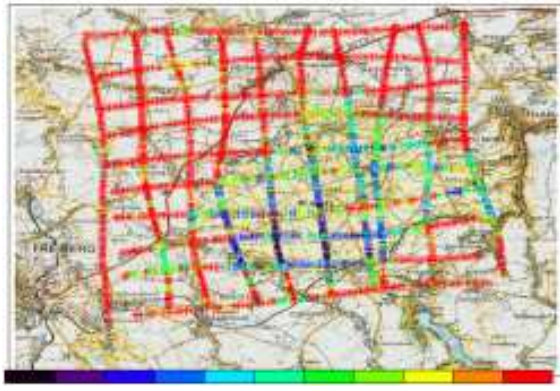


Fig. 8: Grid flight pattern during the Tharandt experiment. This pattern was flown when the convective BL was already established. The difference of wood and grass land is clearly visible by surface temperature (colors) measured by the Do 128 aircraft.

6. THARANDT 2001 EXPERIMENT

During the Tharandt experiment in the framework of the STINHO-1 campaign, no 3D-box pattern but a low-level grid pattern (Fig. 8) was flown with the Do 128 research aircraft. The site consisted mainly of a large forest surrounded by grassland and agriculture. The difference in surface temperature was clearly visible in the infra-red measurements performed by the Do 128. Due to its larger surface roughness it was expected that the forest developed larger sensible heat flux than the surrounding grass, even though the surface temperature of the latter was significantly higher.

To prove this thesis the LLF+IM method was applied to the airborne measurements at about 150 m above the ground (Fig. 9). Although the heat fluxes measured at the flight altitude differed only by a few Wm^{-2} from each other, at the surface the flux above the forest was about 10 Wm^{-2} larger than above the surrounding grassland. This was due to the clearly larger vertical flux gradient, that belonged to the forest. At about 350 m above the ground the extrapolated flux profiles of grassland and wood were united. Whether this is a kind of a turbulent flux blending height will be subject to further research.

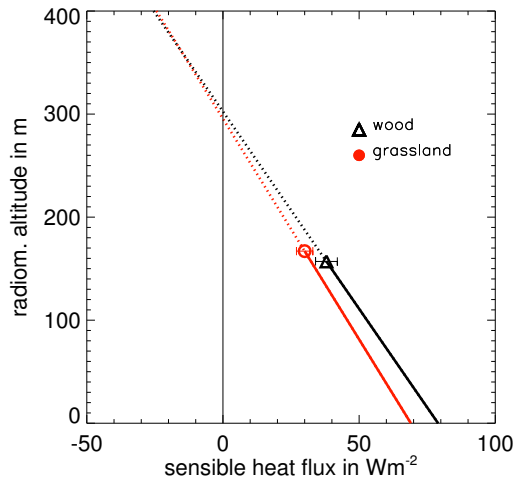


Fig. 9: Vertical turbulent heat fluxes above wood and grassland were determined during the Tharandt 2001 experiment with the Do 128 aircraft.

7. OUTLOOK

There is still a lot of data to analyze: During the LITFASS field experiments in 1997, 1998, 2002, and 2003 the Helipod performed low-level flights above heterogeneous terrain that consisted of forest, grassland, agriculture, and lakes. Various flight patterns were used at different times of the day and under different synoptic circumstances. Among others, one flight pattern will enable the analysis of turbulent fluxes above the individual surface types as in the Tharandt experiment.

The inverse method approach will be extended and improved on further airborne measurements. The next aim is to determine more precise criteria to judge the quality of the calculations, and to apply the method to latent heat and momentum fluxes. The latter includes the difficulties of an obviously not linear profile near the surface and the need of a non-linear inverse model.

The obvious systematic difference in the vertical flux gradients, that is possibly caused by the boundary-layer scaling, will be another topic of future analysis.

ACKNOWLEDGMENTS

We like to thank Jörg Uhlenbrock, Institute for Meteorology and Climatology, University of Hannover, for the Large Eddy Simulations. We are much obliged to the crew of the FJS Helicopter Service in Damme (Germany) who performed the flights with the Helipod, as well as to Rolf Hankers and his Do 128 crew in Braunschweig. The Helipod flights and the field experiments were funded by the German government in several research programs.

REFERENCES

Bange, J., F. Beyrich, and D. A. M. Engelbart, 2002: Airborne Measurements of Turbulent Fluxes during LITFASS-98: A Case Study about Method and Significance. *Theor. Appl. Climatol.*, **73**, 35–51.

Bange, J. and R. Roth, 1999: Helicopter-Borne Flux Measurements in the Nocturnal Boundary Layer Over Land - a Case Study. *Boundary-Layer Meteorol.*, **92**, 295–325.

Beyrich, F., H.-J. Herzog, and J. Neisser, 2002: The LITFASS Project of DWD and the LITFASS-98 Experiment: The Project Strategy and the Experimental Setup. *Theor. Appl. Climatol.*, **73**, 3–18.

Corsmeier, U., R. Hankers, and A. Wieser, 2001: Airborne Turbulence Measurements in the Lower Troposphere Onboard the Research Aircraft Dornier 128-6, D-IBUF. *Meteor. Z., N. F.*, **4**, 315–329.

Engelbart, D. A. M. and J. Bange, 2002: Determination of Boundary-Layer Parameters using Wind Profiler/RASS and Sodar/RASS in the Frame of the LITFASS-Project. *Theor. Appl. Climatol.*, **73**, 53–65.

Grunwald, J., N. Kalthoff, F. Fiedler, and U. Corsmeier, 1998: Application of Different Flight Strategies to Determine Arealy Averaged Turbulent Fluxes. *Beitr. Phys. Atmosph.*, **71**, 283–302.

Hankers, R., 1989: The Equipment of a Research Aircraft with Emphasis on Meteorological Experiments. In: *Soc. of Flight Test Eng., 20th Ann. Symp.*, Reno, Nevada.

Lenschow, D. H., J. Mann, and L. Kristensen, 1994: How Long Is Long Enough When Measuring Fluxes and Other Turbulence Statistics. *J. Atmos. Oceanic Tech.*, **11**, 661–673.

Schröter, M., J. Bange, and S. Raasch, 2000: Simulated Airborne Flux Measurements in a LES Generated Convective Boundary Layer. *Boundary-Layer Meteorol.*, **95**, 437–456.

Tarantola, A., 1987: *Inverse Problem Theory*. Elsevier, Amsterdam, 613 pp.

Wolff, M. and J. Bange, 2000: Inverse Method as an Analysing Tool for Airborne Measurements. *Meteor. Z., N. F.*, **9**, 361–376.

Zittel, P., W. Deierling, and J. Bange, 2002: Using the Inverse Method to Obtain Area-Averaged Turbulent Fluxes from Airborne Measurements at One Low Altitude. In: *15th Conference on Boundary Layer and Turbulence*, AMS, Wageningen, The Netherlands.

Zittel, P., T. Spiess, and J. Bange, 2003: Area-Averaged Turbulent Fluxes from Airborne Measurements over Heterogeneous Terrain using the Inverse Method and MR Cospectra. In: *EGS-EGU-EUG Joint Assembly*, EGU, Nice, France.